Molecular, Spectroscopic, NBO and NLO Properties of 4-Methyl-5-thiazoleethanol: A Comparative Theoretical Study

B. Dede[a,*], D. Avci[b], D. Varkal[c] and S. Bahçeli[c]

[a]Department of Chemistry, Faculty of Arts and Science, Süleyman Demirel University, East Campus, 32260, Isparta, Turkey

[b]Department of Physics, Faculty of Arts and Science, Sakarya University, Sakarya, Turkey

[c]Department of Physics, Faculty of Arts and Science, Süleyman Demirel University, East Campus, 32260, Isparta, Turkey

(Received October 27, 2017; revised version April 20, 2018; in final form September 28, 2018)

In this work, the 4-methyl-5-thiazoleethanol (C_6H_9NSO) molecule was studied by using the experimental spectroscopic techniques (UV-vis in three different solvents and the Fourier transform infrared spectroscopies) and density functional theory calculations. The molecular geometric parameters, vibrational wavenumbers, high-occupied–low-occupied molecular orbitals energies, ^{1}H and ^{13}C NMR chemical shift values, molecular electrostatic potential, natural bond orbitals, and nonlinear optical properties of the 4-methyl-5-thiazoleethanol were performed by using the B3LYP, B3LYP-GD3 and HSEH1PBE levels of density functional theory with 6-311++G(d,p) basis set. The spectral results obtained from the quantum chemical calculations of 4-methyl-5-thiazoleethanol are in a good agreement with the experimental results.

DOI: 10.12693/APhysPolA.134.1083

PACS/topics: 07.60.Rd, 33.20.Tp, 31.15.E–, 42.65.–k

1. Introduction

It is well known that the simplest member of five-membered N,S-heterocyclic derivatives is the thiazole and its structural potential has the biomedical and pharmacological properties. Therefore, thiazoles and their derivatives have attracted the interest over the last decades since they have the varied biological activities such as antifungal, anti-inflammatory, anti-allergic [1–5]. On this content, very recently the 2-ethoxythiazole molecule which is the five-membered heterocycle with one nitrogen atom was investigated using spectroscopic and DFT calculation method [6]. As a continuation of the mentioned study, the 4-methyl-5-thiazoleethanol (C_6H_9NSO) molecule was found to be worth for the investigation based on the biological properties which lead to the use in drug industry by considering the transition metal complexes of heterocyclic thiazoles [7–13]. To our knowledge, there are no quantum chemical studies on the title molecule in the literature. On the other hand, even it is lack of experimental data, for a proper IR and UV-vis spectral understanding and a reliable assignment of all vibrational bands, the density functional theory (DFT) calculations have a powerful quantum chemical tool for the determination of the electronic structure of molecules. On the basis of this fact, the B3LYP-GD3 and HSEH1PBE are the most used levels [14–22].

In the present work, the experimental Fourier transform infrared (FTIR) and UV-vis (in chloroform, ethanol and N,N-dimethylformamide solvents) spectral results and the molecular geometry, the simulated vibrational and UV-vis (in gas phase and chloroform solvent) spectra, the ^{1}H and ^{13}C NMR chemical shift values, the molecular electrostatic potential (MEP), high-occupied–low-occupied molecular orbitals (HOMO-LUMO) and natural bond orbitals (NBO) and nonlinear optical (NLO) properties calculated using DFT/B3LYP, B3LYP-GD3 and HSEH1PBE levels with 6-311++G(d,p) basis set for the 4-methyl-5-thiazoleethanol (C_6H_9NSO) compound were reported.

2. Material and methods

2.1. General information

4-Methyl-5-thiazoleethanol (99%, Sigma-Aldrich), chloroform (99%, Merck), ethanol (99.9%, Merck) and N,N-dimethylformamide (99.8%, Merck) used in this study were obtained from commercial sources and were used without any purification. IR spectrum of the 4-methyl-5-thiazoleethanol was recorded on a Schimadzu IR Prestige-21 FTIR Spectrometer at room temperature with a resolution of 4 cm^{-1} in the transmission mode. The prepared sample was compressed into self-supporting pellet and introduced into an IR cell equipped with KBr window. The ultraviolet visible spectrum of the title compound was recorded by using a PG Instrument T80+ ultraviolet spectrophotometer at room temperature. The ultraviolet visible spectra of the mentioned compound solved in chloroform, ethanol and N,N-dimethylformamide solvents were verified with spectral bandwidth 2 nm and quartz cell 1 cm.

*corresponding author; e-mail: bulentdede@sdu.edu.tr

2.2. Computational details

In this work, all calculations and visualizations were carried out with the Gaussian 09 and GaussView 5 molecular visualization program package on personal computer, respectively [23, 24]. The molecular structure and vibrational computations of 4-methyl-5-thiazoleethanol molecule in ground state were calculated by using DFT/B3LYP, B3LYP-GD3 and HSEH1PBE methods with 6–311++G(d,p) basis set. The wave number values calculated in DFT method contain the systematic errors which come from the negligence of anharmonicity. Besides, these parameters were performed in gas phase of isolated molecule while the experimental measurements were taken in solid phase for the title molecule, and so those are obtained bigger than the observed wave numbers [25]. Therefore, the computed vibrational wave numbers were scaled as 0.961 for frequencies higher than 800 cm^{-1} and 1.001 for frequencies less than 800 cm^{-1} at the B3LYP and HSEH1PBE/6- 311++G(d,p) levels [26, 27]. On the other hand, the assignments of fundamental vibrational modes of the title molecule were verified by using VEDA 4 program on the basis of the potential energy distribution (PED) analysis [28].

NMR calculations were performed in gas phase and chloroform solvent ($\varepsilon = 4.7113$) by using the conductor-like polarizable continuum method (CPCM). ^{1}H and ^{13}C NMR chemical shifts were calculated by employing the gauge-invariant atomic orbital method (GIAO) [29–34].

The calculations of the electronic absorption maximum wavelengths (λ_{max}) in both gas phase and chloroform solvent were verified by using the time dependent DFT (TD-DFT) method at the B3LYP, B3LYP-GD3 and HSEH1BPE/6-311++G(d,p) levels [35, 36]. Furthermore, the NBO and NLO parameters, HOMO and LUMO analysis and molecular electrostatic potential (MEP) of the title compound were calculated at the B3LYP/6-311++G(d,p) level and their 3D plots were performed at the mentioned levels in GaussView 5 program.

3. Results and discussion

3.1. Molecular geometry

The optimized molecular geometry of the title compound obtained at the B3LYP/6-311++G(d,p) level is given in Fig. 1. The bond lengths, bond angles and dihedral angles calculated at the B3LYP (abbr. BB), B3LYP-GD3 (abbr. BG) and HSEH1BPE/6-311++G(d,p) (abbr. HG) levels were presented in Table I. There is no investigation on the crystallographic structure of the title molecule according to our best knowledge.

In Table I, a comparison among the values of the bond lengths, bond angles and dihedral angles for the title compound calculated at the B3LYP, B3LYP-GD3 and HSEH1BPE/6-311++G(d,p) levels shows that the results obtained from the computations are obviously in a good agreement with each other.

TABLE I

Selected calculated bond lengths [Å], bond angles and dihedral angles [°] for 4-methyl-5-thiazoleethanol at the B3LYP, B3LYP–GD3 and HSEH1PBE/6-311++G(d,p) levels

Parameters	BB	BG	HG
Bond lengths [Å]			
C1-S4	1.741	1.743	1.727
C1-H5	1.082	1.082	1.083
C1-N6	1.295	1.295	1.293
C2-C3	1.372	1.371	1.371
C2-N6	1.383	1.382	1.374
C2-C7	1.500	1.499	1.492
C3-S4	1.750	1.748	1.734
C3-C11	1.502	1.500	1.494
C7-H8	1.093	1.093	1.093
C7-H9	1.091	1.091	1.091
C7-H10	1.094	1.094	1.094
C11-H12	1.095	1.095	1.096
C11-H13	1.094	1.093	1.094
C11-C14	1.539	1.538	1.530
C14-H15	1.092	1.092	1.093
C14-H16	1.097	1.098	1.099
C14-017	1.424	1.424	1.412
O17-H18	0.963	0.963	0.960
Bond angles [°]			
S4-C1-H5	120.745	120.812	120.785
S4-C1-N6	114.926	114.928	114.998
H5-C1-N6	124.328	124.259	124.215
C3-C2-N6	115.448	115.461	115.445
C3-C2-C7	126.726	126.412	126.329
N6-C2-C7	117.825	118.126	118.226
C2-C3-S4	109.085	109.223	109.021
C2-C3-C11	129.720	129.182	129.480
S4-C3-C11	121.157	121.486	121.435
C1-S4-C3	89.029	88.943	89.290
C1-N6-C2	111.51	111.442	111.244
C2-C7-H8	110.203	110.246	110.240
C2-C7-H9	112.171	112.085	112.056
C2-C7-H10	110.439	110.315	110.433
H8-C7-H9	108.455	108.533	108.518
H8-C7-H10	107.208	107.315	107.235
H9-C7-H10	108.206	108.199	108.206
C3-C11-H12	108.902	109.202	108.915
C3-C11-H13	110.795	111.153	110.940
C3-C11-C14	113.078	112.136	112.581
H12-C11-H13	106.418	106.532	106.402
H12-C11-C14	109.137	109.186	109.322
H13-C11-C14	108.286	108.460	108.484
C11-C14-H15	109.974	109.763	109.726
C11-C14-H16	109.943	109.693	109.686
C11-C14-O17	112.380	112.407	112.506
H15-C14-H16	107.538	107.520	107.271
H15-C14-O17	105.650	105.874	105.981
H16-C14-O17	111.163	111.400	111.470
C14-O17-H18	109.011	108.958	108.782

TABLE I (cont.)

Parameters	BB	BG	HG
Dihedral angles [°]			
H5-C1-S4-C3	−179.753	−179.519	−179.638
N6-C1-S4-C3	−0.027	0.120	0.029
S4-C1-N6-C2	0.194	0.198	0.209
H5-C1-S6-C2	179.909	179.823	179.863
N6-C2-C3-S4	0.292	0.612	0.437
N6-C2-C3-C11	178.053	177.789	177.526
C7-C2-C3-S4	−179.940	−179.278	−179.722
C7-C2-C3-C11	−2.177	−3.101	−2.633
C3-C2-N6-C1	−0.320	−0.536	−0.426
C7-C2-N6-C1	179.891	179.363	179.720
S4-C3-C11-H12	−153.944	−149.215	−151.492
S4-C3-C11-H13	−37.226	−31.967	−34.702
S4-C3-C11-C14	84.553	89.630	87.087
H12-C11-C14-O17	61.699	61.616	61.802
H13-C11-C14-O17	−53.753	−53.092	−53.838
C11-C14-O17-H18	−67.875	−66.742	−66.833
H15-C14-O17-H18	172.193	173.424	173.253
H16-C14-O17-H18	55.832	56.835	56.862

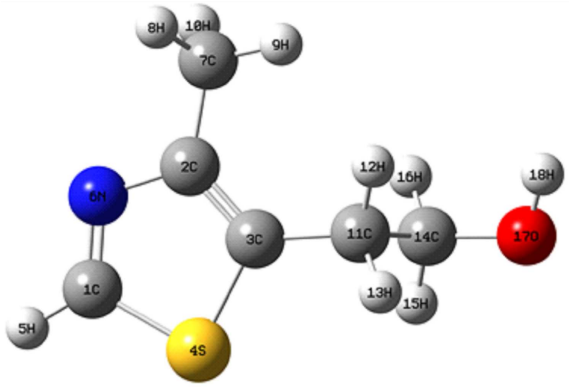

Fig. 1. The optimized molecular geometry of the 4-methyl-5-thiazoleethanol at the B3LYP/6-311++G(d,p) level.

By considering Fig. 1 and Table I, the calculated values at the B3LYP-GD3/HSEH1BPE/6-311++G(d,p) levels for the double C1 = N6 and the single C2–N6 bond lengths in the thiazole ring of the title molecule were found as 1.295/1.293 Å and 1.382/1.374 Å, respectively. These bond lengths of a molecule similar to the structure of the 4-methyl-5-thiazoleethanol were experimentally found to be 1.305 Å and 1.389 Å, respectively [37]. Likewise, the calculated C1-S4 and C3-S4 bond length valued at the mentioned levels were found as 1.743/1.727 Å which were very close to the experimental results (1.725 Å and 1.734 Å), respectively [37]. On the other hand, the C14–O17 and O17–H18 bond lengths at the end of aliphatic chain of the title molecule were calculated as 1.424/1.412 Å and 1.963/1.960 Å (with B3LYP-GD3 and HSEH1BPE/6-311++G(d,p) levels), respectively.

As for the bond angles of the 4-methyl-5-thiazoleethanol compound, the calculated S4–C1–N6, S4–C1–H5, C2–C3–S4, C3–C2–N6 and H5–C1–N6 bond angles at the mentioned levels in thiazole ring were found as 114.928/114.998°, 120.812/120.785°, 109.223/109.021°, 115.461/115.445° and 124.259/124.215°, respectively. These parameters are consistent with those of the 2-ethoxythiazole molecule [6]. However, the C1–S4–C3 bond angle in thiazole ring was calculated as 88.943/89.290° (with the mentioned levels). Moreover, the C14–O17–H18 and H15–C14–O17 bond angles in the chain part of the title compound were calculated as 108.958/108.782° and 105.874/105.981° at the mentioned levels, respectively.

Moreover, according to the changing plane of the molecular structure geometry, the largest and most smallest dihedral angle values calculated at the B3LYP-GD3 and HSEH1BPE/6-311++G(d,p) levels were found as -179.519/-179.638° for H5-C1-S4-C3 and 0.120/0.029° for N6-C1-S4-C3 dihedral angles. By considering all dihedral angles, N6-C1-S4-C3, S4-C1-N6-C2, H5-C1-S6-C2 and N6-C2-C3-S4 dihedral angles in the thiazole ring were calculated as 0.120°, 0.198°, 179.823° and 0.612°. From these calculated angles, the thiazole ring was found to be planar. Furthermore C7-C2-C3-C11 dihedral angle was calculated as -3.101° which indicated that the planarity was preserved along with the first atoms attached to the thiazole ring. But with the C14 and O17 atoms, the planarity of the molecule was distorted and the entire 4-methyl-5-thiazoleethanol molecule was not a planar structure. As a result, the other calculated geometric parameters of title compound in Table I were also in a good agreement with each other.

3.2. Vibrational frequencies

The 4-methyl-5-thiazoleethanol molecule including 18 atoms has 48 fundamental vibrations. The experimental and simulated IR spectra at the DFT/B3LYP and HSEH1PBE/6–311++G(d,p) levels of the title molecule in the region 4000–400 cm^{-1} are shown in Fig. 2. Likewise, the experimental and computed IR vibrational frequencies and their assignments of the 4-methyl-5-thiazoleethanol molecule by using PED analysis are presented in Table II. The OH vibrational stretching mode of the title molecule was observed at 3402.17 cm^{-1} as a broad band and its calculated values at the B3LYP-GD3 and HSEH1BPE/6-311++G(d,p) levels were found as 3681.88/3732.89 cm^{-1} for the title molecule, respectively, as seen in Fig. 2 and Table II [38–43].

The symmetric C–H stretching bands in the ring of title molecule were observed at 3076.46 cm^{-1}, and the same modes for the methyl and methylene were observed at 2945.30 and 2922.16 cm^{-1}, respectively, while the asymmetric C-H stretching mode was observed at 2868.15 cm^{-1} [39–43]. According to PED analysis, these O–H and C–H stretching bands are highly pure modes by varying the interval 100%–83% PED contributions. As seen in Table II, the calculated wave numbers for C–H stretching bands of title molecule at the B3LYP/6–311++G(d,p) level were in a very good agreement with the observed values.

TABLE II

Comparison of FTIR and calculated vibration frequencies for the 4-methyl-5-thiazoleethanol

Mode	Assignments via PED% at B3LYP level	FTIR	Scaled freq. [cm^{-1}][a]		
		[cm^{-1}]	BB	BG	HG
1	ν(OH) 100%	3402.17	3681.88	3681.02	3732.89
2	ν(CH) 100%	3076.46	3086.92	3082.42	3109.27
3	ν(CH) 93%	—	2994.85	2992.50	3023.12
4	ν(CH) 77%	—	2974.95	2973.41	2996.72
5	ν(CH) 98%	—	2963.85	2963.45	2996.35
6	ν(CH) 83%	2945.30	2949.36	2952.20	2975.37
7	ν(CH) 89%	2922.16	2915.67	2913.53	2935.61
8	ν(CH) 88%	—	2911.19	2909.48	2929.69
9	ν(CH) 92%	2868.15	2887.80	2882.41	2903.80
10	ν(CC) 54%	1541.12	1521.34	1523.16	1547.26
11	β(HCH) 83%	—	1452.19	1452.72	1449.14
12	β(HCH) 61%	—	1435.20	1439.23	1447.42
13	ν(NC) 37% + β(HCH) 30%	—	1425.66	1426.04	1429.07
14	β(HCH) 78% + τ(HCNC) 11%	—	1420.13	1419.93	1415.31
15	ν(NC) 35% + β(HCH) 19%	1413.82	1418.25	1417.03	1411.94
16	β(HCH) 83%	1379.10	1359.98	1360.79	1359.11
17	β(HOC) 41% + β(HCH) 14% + τ(HCCC) 20%	—	1354.94	1359.63	1358.35
18	β(HOC) 45% + τ(HCCC) 38%	1334.74	1323.38	1325.23	1329.01
19	ν(NC) 26% + β(CCN) 18% + β(HCN) 18%	1313.52	1289.56	1292.41	1314.05
20	β(HCC) 51%	—	1268.41	1272.42	1269.51
21	τ(HCCC) %42	1242.16	1250.81	1252.61	1253.60
22	ν(CC) 12% + β(HCN) 57%	1195.87	1211.71	1211.85	1216.70
23	ν(NC) 10% + β(HOC) 16% + β(HCC) 17%+ β(HOC) 16%	1155.36	1140.79	1145.20	1153.45
24	ν(NC) 13% + ν(CC) 25%	—	1116.99	1120.42	1128.32
25	ν(OC) 11% + β(HOC) 16% + τ(HCCC) 27%	1053.13	1039.24	1044.97	1057.87
26	β(HCC) 25%+ β(HCC) 52% + γ(CCNC) 11%	—	1016.98	1016.84	1040.82
27	ν(OC) 68% + ν(CC) 16%	—	1010.13	1009.63	1012.15
28	ν(CC) 56%	948.89	971.70	971.41	991.42
29	ν(NC) 19% + τ(HCCC) 40%	920.05	952.01	956.11	955.44
30	ν(CC) 21% + β(CNC) 35%	860.25	878.37	881.40	893.34
31	ν(SC) 19% + β(SNC) 39%	821.68	798.97	800.81	820.83
32	τ(HCNC) 95%	790.81	798.72	798.15	773.38
33	τ(HCCC) 39%	—	778.65	786.39	782.72
34	ν(SC) 10% + β(CCN) 25%	713.66	720.54	726.09	734.95
35	ν(SC) 38% + β(CNC) 15%	663.51	677.40	677.10	692.51
36	τ(CCNC) 32% + γ(CCNC) 13%	644.22	651.42	652.41	657.77
37	ν(CC) 16% + β(SCN) 22% + τ(SCNC) 16%	563.21	558.47	559.65	567.98
38	τ(SCNC) 42% + γ(CCSC) 11%	513.07	526.50	529.05	532.65
39	β(CCN) 38% + β(OCC) 11%	459.06	401.74	404.44	403.76
40	β(OCC) 26% + β(CCC) 14% + τ(SCNC) 14% + γ(CCSC) 10% + γ(CCNC) 16%	—	344.57	346.13	347.80
41	β(CCS) 23%	—	329.94	335.08	335.56
42	β(CCN) 25% + β(CCS) 10% + τ(HOCC) 27%	—	286.76	298.46	290.19
43	β(CCS) 23% + τ(HOCC) 54%	—	279.51	291.25	281.69
44	τ(CCNC) 43% + γ(CCNC) 36%	—	196.80	196.87	198.28
45	β(CCC) 29% + γ(CCSC) 43%	—	109.54	110.64	109.00
46	β(CCS) 12% + τ(HCCC) 13% + τ(OCCC) 66%	—	93.09	102.67	97.68
47	τ(HCCC) 72% + γ(CCSC) 14%	—	88.67	94.19	88.79
48	τ(CCCC) 70%	—	31.69	42.93	39.19

υ — stretching, β — in-plane bending, γ — out-of-plane bending, τ — twisting. [a] The calculated vibrational frequencies of 4-methyl-5-thiazoleethanol were scaled as 0.961 for frequencies higher than 800 cm^{-1} and as 1.001 for frequencies lower than 800 cm^{-1} at the B3LYP and HSEH1PBE/6-311++G(d,p) levels.

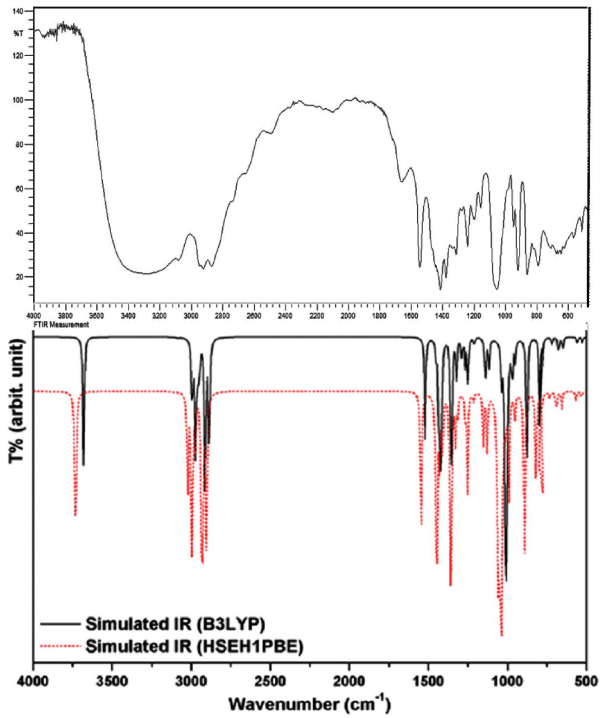

Fig. 2. The experimental and simulated IR spectra of the 4-methyl-5-thiazoleethanol.

The C–C skeletal vibration of the thiazole ring was observed at 1541.12 cm^{-1} as seen in Fig. 2 and the calculated values of this vibrational band at the B3LYP-GD3 and HSEH1BPE/6–311++G(d,p) levels were found as 1523.16 and 1547.26 cm^{-1}, respectively. The observed as the strong peaks at 1413.82 and 920.05 cm^{-1} and the weak band at 1313.52 cm^{-1} in Fig. 2 can be assigned to the C–N stretching mode mixed with the other vibration modes. As seen in Table II, the corresponding theoretical modes were found as 1417.03/1411.94, 956.11/955.44 and 1292.41/1314.05 cm^{-1}.

On the other hand, the observed weak peaks at 821.68 and 663.51 cm^{-1} can be attributed to the C–S stretching bands of the title molecule; these bands were calculated as 800.81/820.83 cm^{-1} [34–39]. Likewise, the strong peak observed at 1053.13 cm^{-1} can be assigned to the C–O stretching mode of the title compound, calculated values at the B3LYP-GD3 and HSEH1PBE/6-311++G(d,p) levels were found as 1044.97/1057.87 cm^{-1}, respectively. Similarly, the middle peak observed at 1379.10 cm^{-1} can be attributed to the H–C–H in-plane bending mode of the title molecule and its calculated values at both level were found as 1325.23/1329.01 cm^{-1}. The other vibrational peaks seen in Fig. 2 can be interpreted by considering the assignments given in Table II [39–43].

3.3. NMR analysis

It is well known that the isotropic chemical shift analysis in the NMR (nuclear magnetic resonance) spectroscopy provides the reliable magnetic properties which satisfy the accurate predictions of molecular geometries and specific NMR signals can be identified and assigned to each hydrogen (and/or carbon, nitrogen) in the molecule [44, 45]. In the framework of the explanations in the computational details section, the ^{1}H and ^{13}C NMR chemical shift values of the 4-methyl-5-thiazoleethanol molecule calculated at the B3LYP-GD3 and HSEH1PBE/6-311++G(d,p) levels in gas and chloroform solvent are given with the order from the largest to the lowest values (see Table III).

TABLE III

The calculated ^{1}H and ^{13}C NMR chemical shifts values (ppm) at the B3LYP, B3LYP–GD3 and HSEH1PBE/6-311++G(d,p) levels for 4-methyl-5-thiazoleethanol in gas (AA) and chloroform (CC)

Atom	BB		BG		HG	
	AA	CC	AA	CC	AA	CC
			^{1}H			
H5	8.42	8.58	8.39	8.55	9.06	9.22
H16	3.74	3.84	3.72	3.81	4.29	4.39
H15	3.58	3.59	3.51	3.51	4.14	4.14
H13	3.14	3.13	3.11	3.10	3.77	3.76
H12	2.77	2.98	2.73	2.94	3.40	3.61
H8	2.55	2.49	2.54	2.49	3.19	3.14
H10	2.47	2.45	2.43	2.41	3.09	3.08
H9	2.14	2.37	2.12	2.35	2.81	3.04
H18	0.19	0.87	0.16	0.85	0.66	1.36
			^{13}C			
C1	158.27	160.47	158.25	160.45	157.75	159.82
C2	156.36	156.89	156.40	156.94	156.75	157.27
C3	139.36	140.68	138.86	140.21	136.82	138.16
C14	70.93	70.95	70.64	70.71	70.36	70.35
C11	36.84	35.96	36.58	35.69	37.31	36.40
C7	16.74	16.55	16.80	16.58	18.66	18.42

The ^{1}H chemical shifts values in gas and chloroform solvent were found at the intervals 8.39-0.16/8.55-0.85 ppm with the B3LYP-GD3/6-311++G(d,p) level and 9.06-0.66/9.22-1.36 ppm with the HSEH1PBE/6-311++G(d,p) level, respectively. The ^{13}C chemical shift values of the title molecule calculated at the B3LYP-GD3 and HSEH1PBE/6-311++G(d,p) levels were found at the intervals 158.25-16.80/160.45-16.58 ppm and 157.75-18.66/159.82-18.42 ppm, respectively. On the other hand, the calculated carbon-13 chemical shift values of C1 and C2 atoms which are bounded to the N atom with high electronegativity in thiazole ring were found as 160.45 and 156.94 ppm at the B3LYP-GD3/6-311++G(d,p) level and as 159.82 and 157.27 ppm at the HSEH1PBE/6-311++G(d,p) level, respectively, in the chloroform solvent as seen in Table III. Likewise, the calculated highest chemical shift value in chloroform solvent for H5 in thiazole ring was found to be 8.55/9.22 ppm. However, the H18 proton which is bounded to the O atom with high electronegativity of the title molecule has the calculated lowest chemical shift value as 0.85/1.36 ppm.

The calculated ^{1}H and ^{13}C NMR chemical shift values of the 4-methyl-5-thiazoleethanol were in good agreement with the values of the similar compound in the literature [46].

3.4. UV-vis absorption and FMOs analysis

The experimental electronic absorption spectra of the 4-methyl-5-thiazoleethanol molecule were recorded in ethanol (EtOH), chloroform ($CHCl_3$) and N,N-dimethylformamide (DMF) solvents. The observed maximum absorption wavelengths (λ_{max}) were recorded at 240, 262, and 321 nm for EtOH solvent, 260 nm for $CHCl_3$ solvent and 273 nm and 328 nm for DMF solvent at the room temperature. The simulated UV-vis spectra of the title molecule in the gas phase and chloroform solvent were calculated by using TD-DFT/B3LYP, TD-DFT/B3LYP and TD-DFT/HSEH1PBE methods with 6-311++G(d,p) basis set. The experimental and simulated spectra of the 4-methyl-5-thiazoleethanol molecule at the mentioned levels are shown in Fig. 3. Furthermore, the experimental (in chloroform solvent) and the calculated λ_{max}, excitation energies and oscillator strengths in gas phase and chloroform solvent at both level are listed in Table IV.

TABLE IV
The theoretical parameters of the electronic transitions and the oscillator strengths (OS) in 4-methyl-5-thiazoleethanol for B3LYP, B3LYP–GD3 and HSEH1PBE/6-311++G(d,p). The experimental value of λ for transition $n \rightarrow \pi^*$ in chloroform solvent is 260 nm.

Chloroform			Gas		
λ [nm]	E [eV]	OS	λ [nm]	E [eV]	OS
B3LYP					
241.21	5.396	0.1703	237.91	5.211	0.112
229.76	5.396	0.0008	234.32	5.291	0.000
226.79	5.467	0.0035	230.07	5.389	0.018
215.76	5.746	0.0064	223.34	5.552	0.003
206.98	5.990	0.0482	208.65	5.942	0.003
206.68	5.999	0.0104	206.69	5.999	0.041
B3LYP–GD3					
241.27	5.139	0.1689	237.84	5.213	0.1102
229.45	5.404	0.0008	233.95	5.299	0.0004
227.67	5.446	0.0027	231.09	5.365	0.0177
216.18	5.735	0.0070	223.92	5.537	0.0038
207.19	5.984	0.0106	208.92	5.935	0.0031
206.49	6.004	0.0488	206.36	6.008	0.0413
HSEH1PBE/6-311++G(d,p)					
235.88	5.256	0.179	232.30	5.337	0.126
224.23	5.529	0.001	228.38	5.429	0.001
220.01	5.635	0.002	223.38	5.550	0.010
208.26	5.953	0.007	215.91	5.742	0.004
201.46	6.154	0.055	201.87	6.142	0.003
199.86	6.204	0.001	201.01	6.168	0.040

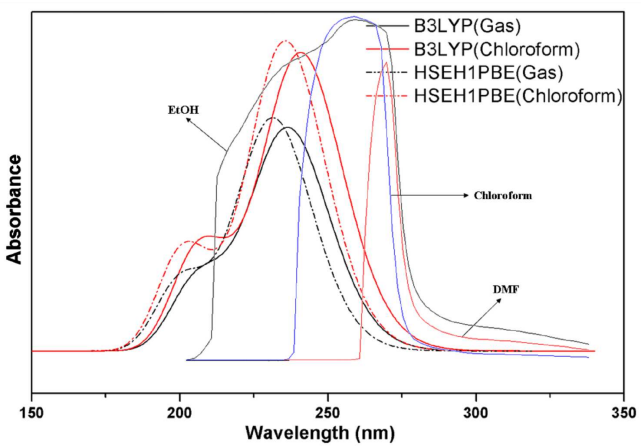

Fig. 3. The experimental (in $CHCl_3$, EtOH and DMF) solvents) and simulated at the B3LYP and HSEH1PBE/6-311++G(d,p) levels UV-vis spectra of the 4-methyl-5-thiazoleethanol.

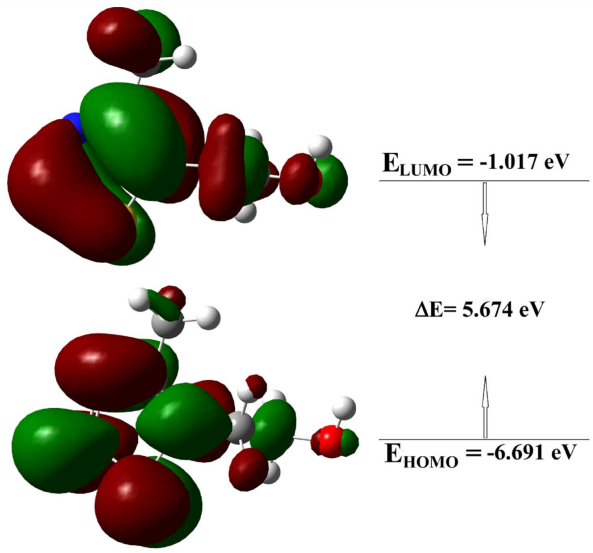

Fig. 4. 3D plots of HOMO-LUMO of the 4-methyl-5-thiazoleethanol at the B3LYP/6-311++G(d,p) level.

The calculated λ_{max} values in $CHCl_3$ solvent were found as 241.27/235.88 nm, at the B3LYP-GD3 and HSEH1PBE/6-311++G(d,p) levels, respectively. Therefore, the observed and calculated absorption bands can be attributed to the $n \rightarrow \pi^*$ transitions for the title molecule [47].

On the other hand, it can be easily stated that the highest occupied molecular orbital (HOMO) implies the outermost orbital filled by electrons and is directly related to the ionization potential and behaves as an electron donor, while the lowest unoccupied molecular orbital (LUMO) means the first empty innermost orbital unfilled by electron and is directly related to the electron affinity and behaves as an electron acceptor. The formed energy gap between HOMO and LUMO called the frontier molecule orbitals (FMOs) indicates the molecular chemi-

cal stability. To determine the molecular electrical transport properties of compounds the formed energy gap can be a critical parameter. Moreover, the molecular properties such as the chemical reactivity, kinetic stability, polarizability, chemical hardness and softness, aromaticity and electronegativity can be determined by using this energy gap [48, 49].

In the result of our calculation, the 3D plots of HOMO-LUMO for the title molecule obtained at the B3LYP/6-311++G(d,p) level is presented in Fig. 4. Therefore, the energy gap between HOMO and LUMO was found as 5.674 eV. By considering Table IV, we can state that this value is in a good agreement with the calculated energy value of 5.396 eV at the B3LYP/6-311++G(d,p) level in chloroform solvent and it corresponds to the $n \rightarrow \pi^*$ transition in UV-vis spectrum of the 4-methyl-5-thiazoleethanol molecule.

3.5. Molecular electrostatic potential

For the understanding of the molecular interactions in a given molecule, the molecular electrostatic potential (MEP) is a crucial tool. Furthermore, the relative reactivity sites for electrophilic and nucleophilic attack, hydrogen bonding interactions, studies of zeolite, molecular cluster and crystal behaviour, investigation of biological recognition and the correlation and prediction of a wide range of macroscopic properties can be interpreted by considering the molecular electrostatic potential [48, 49].

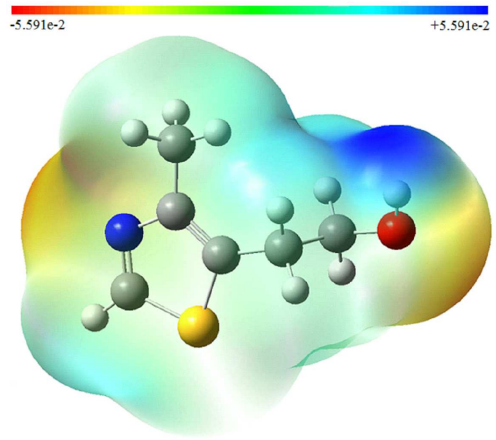

Fig. 5. MEP surface of the 4-methyl-5-thiazoleethanol obtained at the B3LYP/6-311++G(d,p) level.

The 3D plot of the MEP for the 4-methyl-5-thiazoleethanol molecule is exhibited in Fig. 5 obtained at the B3LYP/6-311G++(d,p) level. As seen in Fig. 5, the electrostatic potentials at the surface of the mentioned molecule are shown by different colours. The red colour parts indicate the regions of negative electrostatic potential, the blue sites represent the regions of positive electrostatic potential and the parts with green colour represent the regions of zero potential. Furthermore, the negative regions (red colour) of MEP are related to electrophilic reactivity and the positive ones (blue colour) are related to nucleophilic reactivity. The order for the potential increment can be considered as red $<$ orange $<$ yellow $<$ green $<$ blue. Therefore, the negative regions of MEP surface given in Fig. 5 for the title molecule were localized on the N6 atom in thiazole ring and O17 atom in chain indicating possible sites for electrophilic reactivity due to their electronegative property, while the positive regions of MEP surface were also localized on the protons in title molecule.

3.6. NBO analysis

The natural bond (NBO) analysis stresses the role of intermolecular orbital interaction in the chemical complex and is also a useful and efficient method to grasp the intra- and inter-molecular bondings and interactions among bonds and to study the hyperconjugation interactions or charge transfers (ICT) in molecular systems. In other words, the population analysis can be performed by using the NBO method. This is carried out by considering all possible interactions between the Lewis type (bonding or lone pair) filled orbitals and non-Lewis type (antibonding or Rydberg) vacancy orbitals which are a measure of the intra- and inter-molecular delocalization or hyperconjugation. In this framework, the large $E(2)$ value shows the intensive interaction between electron-donors and electron-acceptors, and greater the extent of conjugation of the whole system. To emphasize the intra- and inter-molecular interactions, the stabilization energies of the title molecule have been investigated by using second-order perturbation theory. For each donor NBO (i) and acceptor NBO (j), the stabilization energy $E(2)$ associated with electron delocalization between donor and acceptor is estimated as [50, 51]:

$$E(2) = -q_i \frac{F_{ij}^2}{\Delta E} = -q_i \frac{\langle i\,|F|\,j\rangle^2}{\varepsilon_j - \varepsilon_i}$$

where q_i is the donor orbital occupancy, ε_i and ε_j are diagonal elements (orbital energies), and F_{ij} is the off-diagonal NBO Fock matrix element. The obtained results of the 4-methyl-5-thiazoleethanol molecule by using the second-order perturbation theory analysis of the Fock matrix at the B3LYP, B3LYP-GD-3 and HSEH1PBE/6-311++G(d,p) levels are presented in Table V.

As seen in Table V, the stabilization energy values greater than 4.13 kcal mol^{-1} of the title molecule are given. Therefore, the strongest first three intramolecular hyperconjugation interactions or intramolecular charge transfers (ICT) were found between π^* antibonding electrons of the double C1–N6 bond and the C2–C3 bond in thiazole ring, the lone pair n electrons of S4 atom and both the C1–N6 and C2–C3 bonds, respectively, by considering the stabilization energy values calculated at the B3LYP, B3LYP-GD-3 and HSEH1PBE/6-311++G(d,p) levels. Similarly, the strong interactions for the 4-methyl-5-thiazoleethanol molecule were also obtained as π(C1–N6) $\rightarrow$ π^*(C2–C3) and n(N$_6$) $\rightarrow$ σ^*(C$_1$–S$_4$) (in Table V).

TABLE V

Second-order perturbation theory analysis of the Fock matrix in NBO basic corresponding to the intramolecular bonds of the 4-methyl-5-thiazoleethanol calculated at the B3LYP, B3LYP–GD3 and HSEH1PBE/6-311++G(d,p) levels. ED — electron density.

Donor (i)	ED(i) [e]			Acceptor (j)	ED(j) [e]			$E(2)^a$ [kcal/mol]			$E(j)-E(i)^b$ [a.u.]			$F(i,j)^c$ [a.u.]		
	BB	BG	HG		BB	BG	HG	BB	BG	HG	BB	BG	HG	BB	BG	HG
σ (C_1-S_4)	1.99	1.99	1.99	$\sigma*$ (C_3-C_{11})	0.02	0.02	0.02	4.13	4.22	4.33	1.09	1.08	1.11	0.06	0.06	0.06
π (C_1-N_6)	1.90	1.90	1.90	$\pi*$ (C_2-C_3)	0.29	0.29	0.30	17.52	17.51	17.56	0.35	0.35	0.35	0.07	0.07	0.07
π (C_2-C_3)	1.86	1.86	1.85	$\pi*$(C_1-N_6)	0.33	0.33	0.34	12.64	12.67	12.04	0.28	0.27	0.27	0.06	0.06	0.05
LP2 (S_4)	1.62	1.62	1.61	$\pi*$ (C_1-N_6)	0.33	0.33	0.34	27.98	27.78	27.18	0.25	0.25	0.25	0.08	0.08	0.07
LP2 (S_4)	1.62	1.62	1.61	$\pi*$ (C_2-C_3)	0.30	0.30	0.30	18.92	18.09	18.63	0.27	0.27	0.28	0.07	0.07	0.07
LP1 (N_6)	1.89	1.89	1.89	$\sigma*$ (C_1-S_4)	0.07	0.07	0.06	14.40	14.44	13.88	0.54	0.56	0.56	0.08	0.08	0.08
LP2 (O_{17})	1.98	1.98	1.98	$\sigma*$ (C_{11}-C_{14})	0.03	0.03	0.03	6.59	6.46	6.65	0.67	0.67	0.67	0.06	0.06	0.06
$\pi*$ (C_1-N_6)	0.33	0.33	0.34	$\pi*$ (C_2-C_3)	0.29	0.29	0.30	59.17	59.18	63.60	0.02	0.03	0.03	0.07	0.07	0.07

[a] $E(2)$ means energy of hyperconjugative interaction (stabilization energy), [b] energy difference between donor and acceptor i and j NBO orbitals, [c] $F(i,j)$ is the Fock matrix element between i and j NBO orbitals.

3.7. Nonlinear optical properties

The magnitudes of total static dipole moment μ, the mean polarizability $\langle\alpha\rangle$, the anisotropy of the polarizability $\Delta\alpha$ and the mean first hyperpolarizability $\langle\beta\rangle$ of the 4-methyl-5-thiazoleethanol molecule calculated at the B3LYP, B3LYP–GD3 and HSEH1PBE/6-311++G(d,p) levels were presented in Table VI. The units for μ in debye, $\langle\alpha\rangle$ and $\Delta\alpha$ in 10^{-24} esu and $\langle\beta\rangle$ in 10^{-30} esu were reported. In this study, we present the values of the μ, $\langle\alpha\rangle$, $\Delta\alpha$ and $\langle\beta\rangle$ as defined [52].

TABLE VI

Total dipole moment (μ in D), the mean polarizability ($\langle\alpha\rangle$, in 10^{-24} esu), the anisotropy of the polarizability ($\Delta\alpha$, in 10^{-24} esu), the mean first-order hyperpolarizability ($\langle\beta\rangle$, in 10^{-30} esu) for 4-methyl-5-thiazoleethanol calculated at the B3LYP, B3LYP–GD3 and HSEH1PBE/6-311++G(d,p) levels

Property	BB	BG	HG
μ	1.20	1.22	1.24
$\langle\alpha\rangle$	14.74	14.73	14.49
$\Delta\alpha$	5.36	6.07	5.15
$\langle\beta\rangle$	2.31	2.41	2.22
$\langle\beta\rangle^a$		0.13	

[a] Taken from Ref. [53]

An important key factor for NLO properties of molecular system is the first hyperpolarizability value (β). For this factor, urea is one of the important compounds used in the investigation of nonlinear optical properties of molecules. Therefore, urea is often used as a threshold value in comparative studies. The β value for urea by using the B3LYP/6-311++G(d,p) level was found as 0.13×10^{-30} esu [53]. In our results, the β values calculated at the B3LYP-GD3 and HSEH1PBE/6-311++G(d,p) levels for the 4-methyl-5-thiazoleethanol molecule, were found as 2.41×10^{-30} esu and 2.22×10^{-30} esu (in Table VI). By comparing these two values it can be stated that β value of the 4-methyl-5-thiazoleethanol molecule is approximately 18.54 and 17.08 times greater than that of the urea at the B3LYP-GD3 and HSEH1PBE/6-311++G(d,p) levels, respectively. These calculated values indicate that the molecule is a good candidate as nonlinear optical material.

4. Conclusion

In the present study, for the 4-methyl-5-thiazoleethanol molecule which has pharmacological and biologic activities, the experimental FTIR and UV-vis (in ethanol, chloroform, and N,N-dimethylformamide solvents) spectra and the analysis of molecular structure and spectroscopic parameters by using quantum chemical computations at the B3LYP, B3LYP-GD3 and HSEH1PBE/6-311G(d,p) levels have been successfully verified. In addition, the vibration frequency and UV-vis data of the 4-methyl-5-thiazoleethanol from the experiments were compared with the values obtained from the two methods of the theory using the basis set of 6-311++G(d,p). In terms of the vibrational frequencies it can be stated that the B3LYP method mostly gives better results. The band observed at 260 nm in the experimental UV-vis spectrum of the title molecule was calculated as 241.27 and 235.88 nm in B3LYP-GD3 and HSEH1PBE/6-311++G(d,p) levels in chloroform solvent, respectively. These values show the high energy ICT transition ($n\rightarrow\pi^*$ transitions) in the title compound. According to NBO results, the high stabilization energy of the title compound is arised from the n electrons localized on the N6 atom in thiazole ring and O17 atom in chain indicating possible sites. In comparison with urea β value, the 4-methyl-5-thiazoleethanol molecule can be candidate for second-order NLO material. Finally, we think that spectral and quantum chemical calculation studies performed by using 4-methyl-5-thiazoletanol molecule will be attractive for researchers working in physical, biological, and pharmacological areas.

References

[1] M. Kurazono, I. Takashi, K. Yamada, Y. Hirai, T. Maruyama, E. Shitara, M. Yonezawa, *Antimicrob. Agents Chemother.* **48**, 2831 (2004).

[2] C.N.R. Rao, R. Venkataraghavan, *Can. J. Chem.* **42**, 43 (1964).

[3] H.S. Sader, D.M. Johnson, R.N. Jones, *Antimicrob. Agents Chemother.* **48**, 53 (2004).

[4] C.M. Moldovan, O. Oniga, A. Pârvu, B. Tiperciuc, Ph. Verité, A. Pîrnău, O. Crişan, M. Bojiţă, R. Pop, *Eur. J. Med. Chem.* **46**, 526 (2011).

[5] A. De Logu, M. Saddi, M.C. Cardia, R. Borgna, C. Sanna, B. Saddi, E. Maccioni, *J. Antimicrob. Chemother.* **55**, 692 (2005).

[6] D. Avcı, B. Dede, S. Bahçeli, D. Varkal, *J. Mol. Struct.* **1138**, 110 (2017).

[7] J. Elguero, A.M.S. Silva, A.C. Tomé, in: *Modern Heterocyclic Chemistry*, 1st ed., Eds. J. Alvarez-Builla, J.J. Vaquero, J. Barlueng, Vol. 2, Wiley-VCH, 2011, p. 635.

[8] M.I. Elzaher, M.M. Kamel, M.M. Anwar, *Pharmazie* **49**, 616 (1994).

[9] A.E. Liberta, D.X. West, *Biometals* **5**, 121 (1992).

[10] F.S. Rodembusch, F.R. Brand, D.S. Correa, J.C. Pocos, M. Martinelli, V. Stefani, *Mater. Chem. Phys.* **92**, 389 (2005).

[11] S. Bondock, T. Naser, Y.A. Ammar, *Eur. J. Med. Chem.* **62**, 270 (2013).

[12] İ. Yilmaz, A. Çukurovalı, *Spectrosc. Lett.* **37**, 59 (2004).

[13] M.J. Kwak, Y. Kim, *Bull. Kor. Chem. Soc.* **30**, 2865 (2009).

[14] F. Jensen, *Introduction to Computational Chemistry*, Wiley, New York 1974.

[15] P. Pulay, *Mol. Phys.* **17**, 197 (1969).

[16] J.P. Perdew, in: *Proc. 21st Annual Symp. on the Electronic Structure of Solids*, Eds. P. Ziesche, H. Eschig, Akademie Verlag, Berlin 1991.

[17] A.D. Becke, *J. Chem. Phys.* **98**, 5648 (1993).

[18] C. Lee, W. Yang, R.G. Parr, *Phys. Rev. B* **37**, 785 (1988).

[19] K. Burke, J.P. Perdew, Y. Wang, *In Electronic Density Functional Theory: Recent Progress and New Directions*, Eds. J.F. Dobson, G. Vignale, M.P. Das, Plenum, New York 1998.

[20] Y. Zhao, J. Pu, B.J. Lynch, D.G. Truhlar, *Phys. Chem. Chem. Phys.* **6**, 673 (2004).

[21] J. Heyd, G.E. Scuseria, M.J. Ernzerhof, *J. Chem. Phys.* **124**, 219906 (2006).

[22] S. Grimme, J. Antony, S. Ehrlich, H. Krieg, *J. Chem. Phys.* **132**, 154104 (2010).

[23] M.J. Frisch et al., Gaussian 09 (now Gaussian 16), Gaussian Inc., Wallingford (CT) 2016.

[24] R. Dennington, T. Keith, J. Millam, *GaussView, Version 5*, Semichem Inc., Shawnee Mission KS, 2009.

[25] J.B. Foresman, E. Frisch, *Exploring Chemistry with Electronic Structure Methods*, Gaussian, Inc., Pittsburgh 1993.

[26] A.C. Costa Jr., G.F. Ondar, O. Versiane, J.M. Ramos, T.G. Santos, A.A. Martin, L. Raniero, G.G.A. Bussi, C.A. Téllez Soto, *Spectrochim. Acta A Mol. Biomol. Spectrosc.* **105**, 251 (2013).

[27] D. Avcı, S. Bahçeli, Ö. Tamer, Y. Atalay, *Can. J. Chem.* **93**, 1147 (2015).

[28] M.H. Jamroz, *Vibrational Energy Distribution Analysis VEDA4*, Warsaw 2004.

[29] F. London, *J. Phys. Rad.* **8**, 397 (1937).

[30] K. Wolinski, J.F. Hinton, P. Pulay, *J. Am. Chem. Soc.* **112**, 8251 (1990).

[31] S. Miertus, E. Scrocco, J. Tomasi, *Chem. Phys.* **55**, 117 (1981).

[32] V. Barone, M. Cossi, *J. Phys. Chem. A* **102**, 1995 (1998).

[33] M. Cossi, N. Rega, G. Scalmani, V. Barone, *J. Comput. Chem.* **24**, 669 (2003).

[34] J. Tomasi, B. Mennucci, R. Cammi, *Chem. Rev.* **105**, 2999 (2005).

[35] R. Bauernschmitt, R. Ahirichs, *Chem. Phys. Lett.* **256**, 454 (1996).

[36] C. Jamorski, M.E. Casida, D.R. Salahub, *J. Chem. Phys.* **104**, 5134 (1996).

[37] J. Jumal, B. Yamin, *Acta Crystallogr. E* **62**, o2893 (2006).

[38] D.L. Pavia, G.M. Lampman, G.S. Kriz, J.R. Vyvyan, *Introduction to Spectroscopy*, Brooks/Cole Cengage Learing, USA 2009.

[39] B.H. Stuart, *Infrared Spectroscopy: Fundamentals and Applications*, Wiley, England 2004.

[40] R.M. Silverstein, F.X. Webster, *Spectroscopic Identification of Organic Compound*, 6th ed., Wiley, New York 1998.

[41] G. Varsanyi, *Vibrational Spectra of Benzene Derivatives*, Academic Press, New York 1969.

[42] L.J. Bellamy, *The Infrared Spectra of Complex Molecules*, 3rd ed., Wiley, New York 1975.

[43] N.B. Colthup, L.H. Daly, E. Wiberley, *Introduction to Infrared and Raman Spectroscopy*, Academic Press, New York 1964.

[44] R.J. Anderson, D.J. Bendell, P.W. Groundwater, *Organic Spectroscopic Analysis*, The Royal Society of Chemistry, Sanderland, UK 2004.

[45] N.E. Jacobsen, *NMR Spectroscopy Explained: Simplified Theory, Applications and Examples for Organic Chemistry and Structural Biology*, Wiley, 2007.

[46] K. Chungkyun, K. Kwark, *J. Polym. Part A* **40**, 4013 (2002).

[47] N. Süleymanoğlu, R. Ustabaş, Y.B. Alpaslan, F. Eyduran, N.O. İskeleli, *Spectrochim. Acta A Mol. Biomol. Spectrosc.* **96**, 35 (2012).

[48] K. Fukui, *Science* **218**, 747 (1982).

[49] R.G. Pearson, *Proc. Natl. Acad. Sci. USA* **83**, 8440 (1986).

[50] C. James, A.A. Raj, R. Reghunathan, V.S. Jayakumar, I.H. Joe, *J. Raman Spectrosc.* **37**, 1381 (2006).

[51] A. Pirnau, V. Chiş, O. Oniga, N. Leopold, L. Szabo, M. Baias, O. Cozar, *J. Vibrat. Spectrosc.* **48**, 289 (2008).

[52] H. Pir, N. Günay, Ö. Tamer, D. Avcı, Y. Atalay, *Spectrochim. Acta A Mol. Biomol. Spectrosc.* **112**, 331 (2013).

[53] P. Dhamodharan, K. Sathya, M. Dhandapani, *Physica B* **508**, 33 (2017).